

1
2
3
4
5
6
7
8
9
10
11
12
13
14
15
16
17
18
19
20
21

Drivers of the fine-scale distribution of a canopy-forming seaweed at the southern edge of its range

Rosa M. Viejo ^{(1)(2)*}, Marisela Des ⁽³⁾⁽⁴⁾, David Gutiérrez ⁽¹⁾⁽²⁾

⁽¹⁾ Área de Biodiversidad y Conservación, ESCET, Universidad Rey Juan Carlos, 28933 Móstoles, Madrid, Spain.

⁽²⁾ Instituto de Investigación en Cambio Global (IICG), Universidad Rey Juan Carlos

⁽³⁾ Centro de Investigación Mariña, Universidade de Vigo, Environmental Physics Laboratory (EphysLab), Campus As Lagoas s/n, 32004, Ourense, Spain

⁽⁴⁾ Stichting Deltares, Boussinesqweg 1, 2629 HV Delft, The Netherlands.

* Corresponding author; email address: rosa.viejo@urjc.es

22 **ABSTRACT**

23 There is growing emphasis on using fine-grained scales to identify the drivers of species geographic range
24 edges, which is essential for predicting the response of species to climate change. This is of particular
25 relevance at the ‘rear-edge’ of species distributions, where higher spatial resolution may also help in the
26 detection of potential refugia for conservation. The southern edge of the range of several canopy-forming
27 algae falls in the NW Iberian Peninsula, where large embayments (rias), influenced by strong upwelling
28 events, may act as contemporary climatic refugia for these key coastal organisms. We investigated the factors
29 driving the fine-scale occupancy patterns of the seaweed *Fucus serratus*, employing a combination of
30 transplant experiments and a fine-grain species distribution model (SDM). Our study revealed that habitat
31 suitability for this species is restricted to particular sites within rias. Transplant experiments showed that
32 germling survival was significantly reduced outside the distribution range. Grazing may limit the species
33 distribution towards the outer sections of rias, where we found the highest densities of grazing gastropods, but
34 not towards the innermost sections. Both winter salinity and autumn seawater temperature were important
35 predictors in the SDM. Our model projections indicate the potential future extinction of *F. serratus* in rias
36 with an increase of 1.5°C in maximum autumn temperature, below the predicted value for this area by the end
37 of the century under the SSP5-8.5 scenario. The results highlight the importance of the autumn season for the
38 performance of this cold-temperate seaweed at the southern edge of its range.

39

40 **Keywords:** distribution patterns, rear-edge of species ranges, canopy-forming seaweed, *Fucus serratus*,
41 climate change, climatic refugia.

42

43

44 1. Introduction

45 Identifying the factors that determine species range edges is a basic and very active research topic in
46 ecology and evolutionary biology (MacArthur 1972, Gaston 2003, Sexton et al. 2009, Willi & Van Buskirk
47 2019). This information is crucial for predicting the response of species to climate change (Sexton et al.
48 2009). Species distribution models (SDMs) are commonly used to investigate the relationship between species
49 ranges and the physical environment (Guisan & Zimmermann 2000). SDMs correlate the current species
50 distribution with climatic and other physical variables and have been widely used to project species ranges
51 under future climates (Pearson & Dawson 2003). However, they have some limitations. For instance, the
52 environment experienced by most species is more heterogeneous than suggested by ecological models, which
53 frequently use medium to coarse-resolution predictors over large geographical areas. The inclusion of finer-
54 scale analysis may be required for a better understanding of the drivers of species range edges and the impact
55 of human-induced global changes (Gillingham et al. 2012, Vale et al. 2014, Lembrechts et al. 2019). This
56 approach is particularly important for organisms in heterogeneous landscapes and/or those whose dispersal is
57 constrained (Hannah et al. 2014).

58 The spatial structure of species range edges at the fine-scale is often complex, formed by a patchy
59 distribution of populations of variable *status* (Gaston 2003, Sexton et al. 2009). The classical view of
60 monotonically worsening conditions from the core to the periphery of species distributions has received mixed
61 empirical support (Sagarin et al. 2006, Dallas et al. 2020, Martin & Canham 2020). Populations close to
62 geographic range edges may indeed occupy patches of benign habitats, i.e. sites with suitable abiotic
63 conditions for the target species (Lennon et al. 2002, Oliver et al. 2009, Ashcroft 2010). Therefore, analysis at
64 higher spatial resolution is also required in order to detect present and future regional and local climatic
65 refugia, which are essential for the conservation of species (Gillingham et al. 2012, Hannah et al. 2014,
66 Lembrechts et al. 2019), especially at the low-latitude, ‘rear-edge’ of species distributions (Hampe & Petit
67 2005).

68 In addition to spatial heterogeneity in climatic and other abiotic conditions, the position and fine-
69 grained structure of range edges may be determined by biotic interactions and dispersal limitations (Holt &
70 Keitt 2000, Case et al. 2005). Sites with suitable physical environments can remain unoccupied at or beyond
71 the range edges due to the influence of these proximate factors, acting independently or in combination (e.g.

72 Bruelheide & Scheidel 1999, Gilman 2006, Stanton-Geddes et al. 2012). Transplant experiments are a
73 powerful way of disentangling the influence of dispersal limitations *versus* habitat quality (including biotic
74 and abiotic factors) on species occupancy patterns (Hargreaves et al. 2014). These experiments directly
75 assessed the vital rates of individuals when moved beyond the range. However, they are difficult to replicate
76 at different spatial and temporal scales in order to sufficiently cover temporal variation in conditions and fully
77 evaluate the demographic performance beyond the range edge (Lee-Yaw et al. 2016).

78 Combining translocation experiments with fine-resolution SDMs can enhance our understanding of
79 the real contribution of multiple factors in establishing species range edges. Thus, SDMs are based on
80 occurrence data, integrating the environmental conditions over larger temporal scales, while transplant
81 experiments reflect current conditions. On the other hand, the distribution of species with poor dispersal may
82 not be in equilibrium with the habitat suitability, and such situations are better captured by transplant
83 experiments. However, studies with the simultaneous use of both approaches remain very scarce (see Greiser
84 et al. 2020 for an excellent example).

85 Large brown seaweeds, mostly kelps and fucoids, play a key role in coastal systems in temperate and
86 Arctic latitudes worldwide, acting as food resources and structural engineers, thus creating habitats for other
87 organisms (Schiel 2006). *Fucus serratus* is one of such canopy-forming macroalgae that dominate
88 Northeastern Atlantic intertidal rocky shores (Lüning 1990). In addition, it is an excellent model of a species
89 with limited dispersal abilities, because it is a dioecious fucoid lacking flotation vesicles, and gamete dispersal
90 is limited to a few meters from the parent plants (Knight & Parke 1950, Arrontes 2002, Coyer et al. 2003).

91 The southern edge of the range of *F. serratus*, like other north Atlantic macroalgae (e.g. *Himanthalia*
92 *elongata* and *Laminaria hyperborea*), falls within the NW Iberian Peninsula, where the distribution is
93 disconnected from the remainder of the northern geographic ranges, with a gap in the inner part of Biscay Bay
94 (Fisher-Piette 1955, Lüning 1990, Arrontes 1993). These southern marginal populations are of great
95 conservation value, as they harbour unique genetic pools resulting from the history of the area as a glacial
96 refugium without any apparent contribution to post-glacial colonization events (e.g. Coyer et al. 2003, Olsen
97 et al. 2010, Neiva et al. 2012). Therefore, the region encompassing these populations is of great importance
98 for coastal conservation while simultaneously facing the imminent threat of climate change (Maggs et al.
99 2008). In fact, in recent decades a westward retraction in the distribution of *F. serratus* and other cold-

100 temperate species (e.g. *F. vesiculosus*, *H. elongata*, *L. hyperborea*, *Saccharina latissima* and *Chondrus*
101 *crispus*) has been detected on northern Spanish shores, constituting a biogeographical shift in entire rocky
102 shore assemblages (Duarte et al. 2013, Fernández 2016, Casado-Amezúa et al. 2019, Muguerza et al. 2022).

103 The NW Iberian Peninsula represents the northernmost limit of the Canary Current Upwelling system
104 (Kämpf & Chapman 2016). Upwelling events are generally stronger along western Atlantic shores, dominated
105 by large embayments or rias, than on the northern coasts of Spain (Fraga 1981, Botas et al. 1990). Therefore,
106 the Atlantic rias within the region of Galicia (NW Spain) may be acting as contemporary climatic refugia for
107 cold-temperate seaweeds (Duarte & Viejo 2018). However, the occurrence of *F. serratus* within the rias is
108 very restricted, even on rocky shores where other intertidal furoids are abundant (Pazó & Niell, 1977,
109 Martínez et al. 2012), and the factors underlying this distribution pattern remain unknown.

110 This study aimed to investigate the factors that influence the fine-scale occupancy patterns of *Fucus*
111 *serratus*, an intertidal canopy-forming seaweed, within two Atlantic rias known to support locally abundant
112 populations of the species (Pazó & Niell, 1977, Duarte et al. 2013). We conducted transplant experiments
113 (replicated in both rias) involving germlings and juveniles, which usually act as bottlenecks to the persistence
114 of seaweed population (Vadas et al. 1992), and we built SDMs to help understand the processes that shape the
115 internal structure of the southern edge of the range of the species.

116 The specific goals of the work were as follows: i) to determine the current distribution patterns of
117 furoid algae within two rias and examine their historical temporal trends; ii) to evaluate whether dispersal
118 limitations or habitat characteristics are the main processes involved in the present-day distribution,
119 considering the potential biotic and abiotic factors involved; and iii) to project the fate of these populations
120 under a future climate change scenario, thereby providing insights into their resilience/vulnerability to the
121 anticipated environmental changes.

122

123 2. Materials and methods

124 A summary diagram of this section is included as Figure S1 of Supplementary material.

125

126 2.1. Study area, occurrence of *F. serratus* and other furoid macroalgae, and environmental variables.

127 The study was conducted in two of the four Rías Baixas, large SW-NE coastal inlets on the western
128 shores of Galicia (NW Spain). Specifically, the work was carried out in the Ría de Muros y Noia (hereafter
129 Ría de Muros) and the Ría de Arousa (Fig. 1; see a brief description of both rias in Appendix S1 of
130 Supplementary material).

131 The historical distribution of *Fucus serratus* within the Rías Baixas during the 1950s-1970s was
132 compiled from previously published articles (Ardre 1957, Donze 1968, Pazó & Niell, 1977). In addition, a
133 detailed field survey was conducted to track the occurrence of *F. serratus* along the coast of NW Spain
134 between 2004 and 2006 (as detailed in Martínez et al. 2012, see also Appendix S1). In particular, a total of 80
135 rocky sites in the Rías Baixas were inspected during low spring tides between May and October 2005, with 51
136 sites located in the targeted rias of Muros and of Arousa (Fig. 1). We repeated the survey inside both rias
137 during the low spring tides in June and October 2011. The occurrence of other intertidal furoid species was
138 also noted, specifically *Fucus vesiculosus*, *F. ceranoides*, *Pelvetia canaliculata*, *Ascophyllum nodosum* and
139 *Himanthalia elongata*. Some locations where *F. serratus* was present in low numbers were subsequently
140 revisited in 2013 and 2020. The species *P. canaliculata*, *A. nodosum*, *F. vesiculosus*, *F. serratus* and *H.*
141 *elongata* may coexist forming successive zones between tide marks from land to sea inside rias, although *A.*
142 *nodosum* is abundant in wave-sheltered shores while *P. canaliculata* and *Fucus* spp. may extend to relatively
143 wave-exposed sites (Ballantine 1961, Donze 1968). Stands of *H. elongata* grow near the low-water mark in
144 more exposed shores, while *F. ceranoides* only occurs in the most estuarine locations (Ballantine 1961, Donze
145 1968).

146 To characterize the environmental variability inside the rias, five physical variables which are
147 biologically meaningful for the target species were considered: seawater surface temperature (SST, seasonal
148 maximum values, and the mean of the coldest month), inorganic nutrient concentration (nitrite and nitrate),
149 surface salinity, wave exposure (significant wave height) and presence/absence of soft sediment. Seawater
150 temperature, salinity and mineral nutrients are amongst the most important variables determining
151 physiological limits to the distribution of seaweeds, in particular furoid algae (Chapman 1995). Furthermore,
152 macroalgal colonization depends on the availability of hard substrata for attachment and wave action (Vadas
153 et al. 1992).

154 Sea surface temperature (°C) was measured *in situ* with Tidbit loggers (resolution of 0.02° C at 25 ° C,
155 Onset Corporation, MA, USA) placed at the mid-shore level in 23 of the 51 surveyed coastal locations (10 in
156 the Ría de Muros and 13 in the Ría de Arousa; see Figure S2 in Supplementary material). The data loggers
157 were attached to the rocky substrate in December 2011, and they recorded temperature every 30 minutes until
158 September 2013. Temperature data were downloaded, and two readings were taken per day coinciding with
159 high tides and thus corresponding to seawater temperatures. Some gaps in the data set were generated by
160 mechanical failure or loss of data loggers due to human interference. Therefore, parts of the seawater
161 temperature time series provided by some loggers had to be interpolated (see method in Appendix S1).
162 Despite these gaps, the completeness of temperature data averaged 89 and 93% in Ría de Arousa and Muros
163 respectively (range: 43 to 100%),

164 Seawater seasonal maximum temperatures were calculated per location as the average of maximum
165 daily values (i.e. taking the highest value of the two readings per day) in the corresponding months (January to
166 March, April to June, July to September and October to December) for the period December 2011 to
167 September 2013. The mean temperature of the coldest month (i.e. mean seawater temperature, considering the
168 two daily readings of the coldest month each year) was also calculated for the same period.

169 Dissolved inorganic nutrients (nitrate plus nitrite, μM) were measured at 18 sampling stations within
170 the rias (Figure S1 in Supplementary Material). The data were collected at approximately weekly intervals in
171 2012-2013 by the *Instituto Tecnológico para o Control do Medio Mariño de Galicia* (INTECMAR, Xunta de
172 Galicia, Vilagarcía de Arousa, Spain; <http://www.intecmar.gal/>). Surface nutrient concentrations were
173 calculated by integrating values from 0 to 15 m. The lowest values of inorganic nutrient concentrations during
174 the year were recorded in summer. The summer (July-September) mean value was calculated for 2012-2013.

175 Salinity was computed using the hydrodynamic numerical model Delft3D-Flow
176 (<https://oss.deltares.nl/web/delft3d>). The numerical simulations were conducted using a previously
177 implemented and validated mesh and parametrization designed explicitly for the *Rias Baixas*, as described by
178 Des et al. (2019, 2020; see these articles for a detailed description of the model configuration). Model
179 simulations cover the period January-February 2012-2013, with a spatial resolution of 150 x 200 m in the
180 inner part of the rias. These months typically correspond to the highest river discharges in the region (Otero et

181 al. 2010), resulting in minimal annual salinity values and significant spatial variability within rias. Model
182 outputs were recorded every six hours, and mean salinity was calculated.

183 Significant wave heights at high resolution inside rias were obtained from a model of Galician shores
184 available from MeteoGalicia (Galician wave atlas, www.meteogalicia.gal/modelos/). This model uses
185 historical deep waters wave data series from 1958 to 1999 from the SIMAR-44 data set (www.puertos.es)
186 covering from 1958 to 1999 and propagates these waves into the rias. The model uses a mesh of 75 m near the
187 coast and even higher resolution in shallow waters (see details in the Galician wave atlas, MeteoGalicia). The
188 99th percentile significant wave height (H_{s99}), and the significant wave heights associated with a 10-year return
189 period ($Rt10-H_s$) were chosen as representative of extreme values within rias.

190 The presence/absence of soft sediment covering the rocky substratum was determined for each
191 location by visual inspection during the field survey and also by examination of aerial orthophotos obtained
192 from the National Geographic Institute of Spain
193 (<https://centrodedescargas.cnig.es/CentroDescargas/index.jsp#>).

194

195 2.2 Transplant experiments

196 Three rocky locations were selected from those visited during the field survey per ria (in total, six
197 locations) to conduct transplant experiments with two early stages of development of *F. serratus*: microscopic
198 germlings and juveniles. In both rias, an ‘origin location’, where *F. serratus* is abundant and persistent over
199 time (see results of field surveys) was selected. One of the other two locations was placed following the origin
200 location as a reference moving to the outside, and the other towards the inside of the ria. Outer and inner
201 locations were selected where the target species *F. serratus* was absent but where other furoids (*F.*
202 *vesiculosus*, *A. nodosum* and *H. elongata*) were relatively abundant at mid-shore levels.

203 The locations were respectively Isla de Arousa, Lobajera-Chan and Tanxil, selected as origin (O),
204 exterior (E) and interior (I) locations in the Ría de Arousa, and O Freixo, Punta Avelleira and Punta Barquiña
205 selected as O, E and I locations in the Ría de Muros (Fig. 1).

206

207 To characterize the biotic environment of the selected locations for the transplant experiments, the
208 abundance of *F. serratus* was estimated, along with that of other intertidal furoids (*F. vesiculosus*, *A.*

209 *nodosum*, *H. elongata*) and macrograzers, at each of the six locations (see above). Sampling was conducted
210 during low spring tides, at approximately 1.4 m above the Lowest Astronomical Tide (LAT), corresponding to
211 the middle of the zone dominated by *F. serratus* in origin locations, in May 2012 to estimate algal cover, and
212 May and July 2012 to count grazers. At each location, three sites, each separated by a distance of about 10-20
213 m, were established, and four plots per site (0.25 m² for algae, and 0.09 m² for grazers) were randomly chosen
214 for estimation of algal cover and density of grazers (see methods in Appendix S1).

215 Artificial discs with a rough surface (4 cm in diameter) were used for settlement of *F. serratus* in the
216 field (see details of the making procedure in Appendix S1). A total of 10 plates with four discs each (i.e. 40
217 discs) were fastened to rocky platforms in the ‘origin’ locations of both rias during the low spring tides of
218 September 2012 and were removed two months later, during spring tides in November 2012. The plates were
219 fixed at mid-shore level (about 1.4 m above the LAT) below the *F. serratus* canopy and separated by a
220 minimum distance of 1-3 m from each other.

221 A subsample of 23 discs per location was examined under a stereo microscope within hours after
222 collection to count the number of germlings in November. Discs were placed in aerated sea water and returned
223 to the field the same night or the following day. Eight of the initial 80 discs were discarded due to low
224 recruitment values. In each ria, 12 randomly chosen discs were transplanted to the outer location and 12 to the
225 inner location, and the remaining 12 discs were returned to the origin location as ‘self-transplants’. In inner
226 and outer locations, plates with discs were fixed under furoid canopies at tidal heights similar to the origin
227 locations. Additionally, 6 clean discs were fixed in the origin and inner locations to monitor any new
228 settlement (control discs). Due to logistic constraints, this was only done in the Ría de Muros. The transplant
229 experiment ran for 2 months (until January 2013), after which the discs were collected, and the recruits were
230 counted under a stereo microscope. Some discs were lost resulting in a final number of discs per location
231 ranging from 7 to 12.

232 During the experiment, we observed development of reproductive structures (receptacles) in
233 individuals of *F. serratus* in origin locations and *A. nodosum* in inner locations, but scarcely in plants of *F.*
234 *vesiculosos* in outer locations. New settlers were recorded on the control discs placed in the origin location
235 (underneath *F. serratus* canopy), but none in the inner location (under a cover of *A. nodosum*). The new

236 settlement was subsequently considered when analyzing the results of the experiment (see the analyses section
237 below).

238 Transplant experiments with juveniles (i.e. non-reproductive individuals of <15 cm length) were
239 conducted at the same locations as the germling transplantations during short periods (2-3 months) to prevent
240 the accidental introduction of *F. serratus* at sites where the species was historically absent. These experiments
241 were conducted during two different periods throughout the growing season of *Fucus serratus* (Arrontes
242 1993): February to May 2012 in the Ría de Arousa, and March to May 2012 (first trial) and beginning of June
243 to the end of July 2012 (second trial) in the Ría de Muros.

244 In the origin locations, in each trial we removed 54 of 72 selected juveniles (we left 18 untouched),
245 along with a fragment of the bedrock, mussel shells (*Mytilus galloprovincialis*) or barnacles (*Balanus* sp.) to
246 which juveniles were firmly fixed. The specimens were carefully removed with a hammer and chisel to
247 prevent damage to the fronds. Detached individuals were randomly assigned to treatments and either
248 transplanted back to the same origin location (procedural controls, hereafter named ‘self-transplants’) or to
249 outer and inner locations at mid-shore levels, about 1.4 m above LAT (n = 18). Self-transplants and
250 transplants were numbered with a plastic label and cemented onto the rocky substratum. Unmanipulated
251 juveniles in origin locations were also labelled and used as controls (n = 18). At inner and outer locations,
252 transplantations were arranged in three groups of 6 juveniles each, placed at randomly selected sites of about 1
253 m² and separated 3-5 m from each other. By contrast, in the origin locations, the three groups included 12
254 individuals (6 self-transplants plus 6 controls). Self-transplants were subjected to similar transportation times
255 and conditions to those of the other transplanted individuals to ensure adequate procedural controls for the
256 transplanting process. The final design was, however, unbalanced, due to problems with attachment of the
257 samples. In particular, the transplanted individuals in the outer location of Ría de Arousa from the first trial,
258 and those in the inner location of Ría de Muros from the second trial were missing.

259 At the beginning and at the end of each experimental trial, the length of the thalli (from the base of the
260 holdfast to the tip of the longest branch) and the maximum circumference were measured to within 0.1 cm.
261 For circumferences <2 cm, an approximation of 2 cm was used. The volume of each individual (v) was

262 calculated as $v = lc^2$ (l = length, c = circumference, Åberg 1990). At the end of the experiments, the juveniles
263 from the different treatment groups were collected, dried at 60 °C for 48 hours and weighed.

264

265 *2.3 Statistical analyses*

266 The abundance and species composition of fucoids and grazers (expressed as percent cover and
267 density, respectively) were analyzed using general mixed linear models (analyses of variance, ANOVAs). Ria
268 (two levels) and Location (three levels: origin, interior, exterior) were treated as fixed and orthogonal factors,
269 and Site (three sites per location) as a random and nested factor within the interaction of Location x Ria. A
270 third fixed and orthogonal factor, Date (with two levels), was included in the previous design to test for
271 differences in grazer densities.

272 Differences between Rias and Locations (as fixed and orthogonal factors) in the final counts of
273 germlings were analyzed using a generalized linear model (GLM) with a negative binomial distribution and a
274 log link function. The negative binomial was used instead of the Poisson distribution owing to the presence of
275 data overdispersion (dispersion parameter = 15.17; Zuur et al. 2009). The analysis was performed after
276 subtracting the average number of new settlers recorded on the new control discs (see the experimental set up)
277 from the counts of origin locations.

278 Data from juvenile transplants were analyzed by one-way ANOVAs, with Treatment as a fixed factor
279 (four levels: self-transplants, controls, inner transplants and outer transplants). The dependent variables were
280 the initial length and volume, elongation (final - initial length) and final dry weights. Separate analyses were
281 conducted for each trial and ria due to differences in starting dates and the unbalanced design resulting from
282 loss of transplants.

283 Homogeneity in the spread of residuals was checked graphically using coplots of standardized
284 residuals versus fitted values. Cochran's C-tests were also used to test the assumption of homogeneity of
285 residuals in ANOVAs with balanced data. The statistical significance of the analyses was defined at $p = 0.05$.
286 All analyses were executed in R public domain package (R Core Team, 2014). ANOVAs with mixed (fixed
287 and random factors) and nested designs were performed with the GAD package (Sandrini-Neto & Camargo,
288 2014) in R.

289

290 2.4 *Species distribution models*

291 Seawater temperature data obtained *in situ* in 23 rocky coastal locations were interpolated to produce
292 values at all the 51 sites of the field survey where the occurrence of *F. serratus* and other fucoids was
293 recorded. The information was processed with the Geographical Information System (GIS) software ArcGIS
294 (version 10.5). Maps of the study area were obtained in format Shapefile (vector data) as BCN200 (*Base*
295 *Cartográfica Numérica* scale, 1:200,000) from the National Geographic Institute of Spain
296 (<https://www.ign.es/web/ign/portal>). The data were interpolated using the inverse-distance weighted-
297 interpolation algorithm (IDW) with power 2 (Euclidean distance), 2 points, and a size cell of 500 x 500 m.
298 IDW is considered an appropriate method for spatial interpolation of SST (Kusuma et al. 2018). In the case of
299 the three outermost external sites on the northern coast of Ría de Muros, we used the two facing sites at the
300 southern coast for interpolations (see Figure S2 in Supplementary materials), instead of the most proximate
301 locations from the same northern coastal line. This decision was made because the nearest locations were
302 environmentally very distinct, situated in a very shallow and wave-sheltered small bay (Muros bay) which had
303 the warmest recorded temperatures of both rias.

304 Summer average nutrient concentrations (nitrite+nitrate) obtained from INCTEMAR in sampling
305 stations inside rias were interpolated to our coastal sites by the IDW method explained above. The salinity and
306 significant wave heights in the targeted coastal locations were extracted from the respective high-resolution
307 models (see section 2.1 above).

308 To analyze the relationship between environmental parameters and occurrence of *F. serratus* inside
309 the rias, we applied generalized linear models (GLMs) with a binomial distribution and a logit link function
310 (Zuur et al. 2009), as both presence and absence data were reliably determined in the field surveys. Seasonal
311 maximum sea temperatures, mean summer nutrient concentrations and mean salinity in January-February
312 (representing in both cases minimal annual values of the variables), significant wave heights (H_{s99} and $Rt10-$
313 H_s) and type of substratum (presence/absence of mud) were pre-selected as meaningful predictors, based on
314 previous ecological knowledge on environmental limiting factors for the species (e.g. Arrontes 1993,
315 Chapman 1995, Malm et al. 2001, Chapman et al. 2002). As final distribution models previously constructed

316 for the target species at broader spatial scales included the mean SST of the coldest month (e.g. Jueterbock et
317 al., 2013), we also incorporated this variable in alternative full models (see below).

318 A dummy variable was created with the zero-value assigned to those rocky locations with presence of
319 continuous muddy cover.

320 Pairwise Pearson correlation coefficients for these variables were examined prior to the final selection
321 of predictors. Correlations between spring and summer, spring-autumn, summer-autumn and summer-winter
322 maximum seasonal temperatures were significant, reaching >0.7 in absolute value (the commonly applied
323 threshold for collinearity, see Dormann et al. 2013). The same occurred with winter maximum temperatures
324 and the mean of the coldest months, or the two variables of significant wave heights, i.e. H_{s99} , and $Rt10-H_s$
325 (Pearson correlation = 0.97). Thus, only one of these paired correlated variables was included in alternative
326 full models. Despite the small spatial scale analyzed, we fitted all possible combinations of linear and
327 quadratic terms, based on the potential biological meaning of quadratic responses (e.g. the target species is
328 typical from shores with intermediate values of wave exposure, i.e. semi-exposed to wave action, Ballantine
329 1961). The Akaike Information Criterion (AIC) was used to rank models, and model selection was performed
330 with the ‘MuMIn’ package (Barton 2012, R Development Core Team 2014). The differences in AIC values
331 between each model and the model with the minimum value ($\Delta_i = AIC_i - AIC_{min}$) were calculated. The best
332 model(s) was(were) selected from the total collection, following these criteria (Richards et al. 2011): i) the
333 subset of candidate models included those with the lowest AIC values and $\Delta_i \leq 6$; and ii) within this subset, the
334 model(s) which did not have simpler variants was(were) selected. This rule ensured a high probability of
335 selecting the most parsimonious models.

336 We tested for spatial autocorrelation, which can influence the reliability of statistical analyses because
337 it potentially generates more complex models in theoretical approaches (Diniz-Filho et al. 2008, see details in
338 Appendix S1).

339 The explained deviance of the selected model/s, which is similar to R^2 in a linear regression, was
340 calculated as $100 \times \frac{Null\ Deviance - Residual\ Deviance}{Residual\ Deviance}$ (Zuur et al., 2009). Model performance was tested using
341 jackknife partitioning techniques (Fielding & Bell 1997, Guisan & Zimmermann 2000, see details in
342 Appendix S1). Relative true presences or sensitivity of the model (RTP), relative true absences or specificity

343 (RTA), and the kappa coefficient (k) were calculated. The prevalence of *F. serratus* (i.e. the ratio of observed
344 presences to the total number of surveyed sites) was used as the threshold probability to calculate these
345 performance metrics (Fielding & Bell 1997). Model performance was additionally tested using the area under
346 the curve (AUC) of a receiver operating characteristic (ROC) plot (Fielding & Bell 1997). The AUC was
347 calculated using the jackknife scores with the R package pROC (Robin et al. 2011).

348 We also separately analyzed the relationship between the presence/absence of fucooids (considering all
349 the species together) and significant wave heights, and between the occurrence of *F. serratus* and each of the
350 other fucooid species, by applying univariate generalized linear models (GLMs) with a binomial distribution
351 and a logit link function.

352

353 2. 5. *Distribution projections under a future climate change scenario*

354 The distribution of *F. serratus* in the rias was significantly correlated with autumn seawater
355 temperature and winter salinity (see Results). Rather than making precise projections, we aimed to explore
356 potential trends in the future distribution of the target species in the rias, based on changes in these
357 parameters. With this purpose, we used historical seawater temperature anomalies reported for the last few
358 decades (1990-2018) by Barrientos et al. (2020) in the Ría de Muros. These authors estimated a yearly
359 increase of 0.022°C in autumn (*in situ* data weekly measured by INCTEMAR). Assuming this warming trend,
360 we considered a scenario with an increase in autumn SST of 1.5°C, simulating the value reached in this season
361 approximately by the end of this century (in 2083, i.e. 70 years since 2013).

362 For salinity data, we obtained projected mean values of January-February for the period 2080-2089
363 under the RCP8.5 greenhouse gas emission scenario. Salinity was again computed using the hydrodynamic
364 numerical model Delft3D-Flow (<https://oss.deltares.nl/web/delft3d>), and numerical simulations were
365 conducted using the mesh and parametrization designed explicitly for the Rías Baixas, as described by Des et
366 al. (2019, 2020).

367 Finally, we fed our predictive model with the projected temperature and salinity data to obtain future
368 species occurrence patterns. The present prevalence of *F. serratus* was again used as the threshold probability.

369

370 3. Results

371

372 3.1 *Historical and current distribution of Fucus serratus in the Rías Baixas*

373 Only four sparse but relatively abundant populations of *F. serratus* had previously been documented
374 on the rocky shores of the Rías Baixas between the 1930s and 1970s: O Freixo in Ría de Muros, Isla de
375 Cortegada in Ría de Arousa, and Meira and Moaña in the Ría de Vigo, the southernmost of the Rías Baixas
376 (Miranda 1934, Ardré 1957, Donze 1968, Pazó & Niell 1977). At least two of the cited sites, O Freixo and
377 Moaña, have continued to harbour persistent populations since 1960 to the present day (Pazó & Niell 1977,
378 Martínez et al. 2012, this study).

379 Detailed surveys conducted in 2005 in the Ría de Muros and Ría de Arousa and described by
380 Martínez et al. (2012) showed that fucoids dominated a large part of intertidal rocky shores of the rias.
381 However, the presence of *F. serratus* was only recorded in 12 of 51 sites visited, forming a narrow fringe
382 along the rias (Fig. 1; see Table S1 for the list and coordinates of sites; see also Fig 2b in Martínez et al.,
383 2012). In the other two rias in the Rías Baixas (Ría de Pontevedra and Ría de Vigo), the presence of *F.*
384 *serratus* was testimonial. Only one population, although abundant, was detected on the north coast of Ría de
385 Vigo (the above-cited Moaña), from the 29 surveyed sites (data from Martínez et al. 2012). Miranda (1937)
386 reported a total absence of *F. serratus* in the Ría de Pontevedra. Thus, most of the populations of *F. serratus*
387 in the Rías Baixas are concentrated in the target rias of Muros and Arousa. In our subsequent surveys in 2011
388 and 2020, *F. serratus* populations remained apparently unchanged, except in Río Azor, located on the north
389 side of Ría de Arousa (Fig. 1), where the species was already scarce in 2005, with only a few disperse plants,
390 which had disappeared by 2020. Hence, this location was considered an absence record when constructing the
391 distribution model.

392

393 3.2 *Transplant experiments*

394 The composition of fucoid cover clearly differed between the locations used for the transplant
395 experiments, although there were similarities between rias. In the ‘origin’ locations of both rias, *Fucus*
396 *serratus* and *F. vesiculosus* co-dominated, with presence of patches of *Himanthalia elongata* (and
397 *Ascophyllum nodosum*, in the Ría de Muros, see Fig. 2a). At similar tidal heights, *F. vesiculosus* monopolized
398 the space in the outer locations of both rias, unlike in the areas where *F. serratus* was present. In inner

399 locations either *A. nodosum*, or *A. nodosum* and *F. vesiculosus* dominated (Fig. 2a). Despite these changes in
400 species composition, the total cover of furoids did not differ significantly among locations or rias, but varied
401 at small spatial scales (Table 1a, significant effect of Site).

402 The density of grazers, however, increased from inner to outer locations, and the gradient was sharper
403 in the Ría de Muros than in the Ría de Arousa (Figure 2b, Table 1b, significant interaction Ria x Location;
404 SNK test). This difference occurred despite the shorter linear distances between sites in the first ria (Fig 1).
405 There was also significant variability at a small scale (Table 1b, Site effect). The dominant grazing species
406 differed between rias. In Muros, the most abundant taxa were periwinkles of the genus *Littorina* and topshells
407 of the genera *Steromphala* and *Gibbula*. By contrast, in the exterior and origin locations of Arousa another
408 topshell, *Phorcus lineatus*, and limpets from the genus *Patella* were abundant, in addition to *Littorina* and
409 *Steromphala* (Fig. 2b). The dominant species of the genus *Steromphala* was *S. umbilicalis*. Another two
410 congeneric species, *S. pennanti* and *S. cineraria*, were present, along with *Gibbula magus*, but at much lower
411 densities (the latter species was only detected in Ría de Muros). The chiton *Acanthochitona crinita*, although
412 present, was also very rare.

413 Just before transplantation (in November), the number of embryos settled on each disk was 178 ± 19
414 (mean \pm SE, $n = 46$), and there were no significant differences between the rias (ANOVA for Ria effect, $F_{1,44}$
415 = 0.44, $p = 0.509$). Two months after transplantation, the average number of surviving germlings was
416 significantly higher in the original location than in the outer and inner locations (Fig. 3; Table 2 a, b,
417 significant difference between origin and exterior/interior locations, $p = 0.007/0.013$). There was a non-
418 significant trend for these differences to be greater in Ría de Muros, with higher survival rates in the origin
419 location of O Freixo (Fig. 3, Table 2 a, interaction Ria x Location, $p = 0.07$).

420 In the juvenile transplant experiments, the initial sizes of specimens (length and volume) did not differ
421 among treatments (i.e. self-transplant, control, exterior and interior) in any trial (see analyses in Table S2 of
422 Supplementary material). However, initial sizes differed between rias in the first trial, with larger juveniles in
423 Arousa than in Muros (Table S2, mean length \pm SE = 10.3 ± 0.2 cm in Arousa and 9.5 ± 0.3 cm in Muros;
424 volume: 75.9 ± 5.3 and 60.2 ± 4.4 cm³ respectively, $n = 72$). In the second trial, the mean values of initial
425 length and volume were $8.7 (\pm 0.2)$ cm and $67.2 (\pm 4.3)$ cm³ ($n = 144$).

426 We detected a marginally significant effect of the experimental manipulation, with lower elongation
427 values in self-transplants than in controls (first trial in ria of Arousa, second trial in Muros, see Fig. 4 a,c;
428 Treatment effects $p \sim 0.05$). However, no significant differences were detected in either elongation or final
429 weight of juveniles among transplantation treatments (Fig. 4).

430 In the second trial, most of the juveniles transplanted to the exterior location (10 out of 12 individuals)
431 in the Ria de Muros presented evident grazing marks, while they were very rare in control and self-transplants
432 (3 out of 20 plants, see also Figure S3).

433

434 3.3 *Habitat distribution model of *F. serratus* inside rias. Projections under future climate change* 435 *scenario*

436 Alternative initial full models that included seawater temperatures in spring, summer or winter, or the
437 mean of the coldest month, yielded much higher AIC values (>42) than the model including the autumn
438 values (AIC ~ 29 , see Table 3). Models including either H_{s99} or $Rt10-H_s$ as wave height variables behaved
439 similarly, although with slightly lower AIC values for H_{s99} alternatives. Therefore, we started with a full
440 model incorporating autumn seawater temperature and the other predictors of nutrient, salinity, wave height
441 (H_{s99}) and substrate.

442 Among the selected subset of 25 models with $\Delta i \leq 6$, only one was the “best” (Table S3), according to
443 the defined criteria of lower AIC values and simplicity (see methods). This model linked *F. serratus*
444 occurrence to maximum autumn seawater temperatures and salinity in January-February (Table 3). Species
445 occurrences were associated with lower temperatures and intermediate salinity (Figs. 5 and 6; quadratic
446 response to salinity, see Table 3). Specifically, the species was absent at those sites with autumn maximum
447 temperature $>16.6^\circ\text{C}$ and with mean salinity <33 , with a greater probability of occurrence at salinity >33 and
448 <35 , particularly in the range 33-34 (Fig 5). The correlogram of the model was not globally significant,
449 suggesting that spatial autocorrelation in the residuals from the distribution model was negligible. The
450 explained deviance of the model was $\sim 60\%$ (Table 3), and it correctly predicted high proportions of both
451 presence and absence of the species (values of RTP and RTA in Table 3). The discrimination ability using the
452 kappa coefficient was classified as ‘good’, and by means of AUC value, as ‘high’ (Table 3).

453 The occurrence of *F. serratus* within the rias was not negatively correlated with the presence of any
454 other furoid. However, it was positively linked to the distribution of *H. elongata* (significant univariate
455 logistic regression: $p < 0.001$ and 0.03 for intercept and parameter estimates respectively, parameter estimate =
456 1.58). The occurrence of intertidal furoids (considering all the species together: *F. serratus*, *F. vesiculosus*, *F.*
457 *ceranoides*, *H. elongata*, *A. nodosum* and *P. canaliculata*) was negatively related to wave height (significant
458 univariate logistic regression, $p < 0.001$ for both intercept and parameter estimates, parameter estimate = -
459 1.37).

460 Regarding the future climate change scenario, the projection suggests that *F. serratus* is likely to
461 become extinct in the rias (with occurrence probabilities $< 1 \times 10^{-14}$ at any site) when an increase of 1.5°C was
462 applied relative to present SST autumn temperatures and the projected salinity under RCP8.5 (see methods).
463 Under this scenario, all sites had maximum autumn temperatures well above 16.6°C , while the number of
464 locations with salinity values in the range of 33-35 increased from 8 to 42.

465

466 **4. Discussion**

467 Our study revealed that habitat suitability for *Fucus serratus* is very limited inside the Atlantic rias in
468 the NW Iberian Peninsula. The potential contemporaneous refugium for this canopy-forming species in rias is
469 thus restricted to specific sites, with several biotic and abiotic post-settlement filters shaping the internal
470 structure at the southern edge of the species range.

471 Germling survival was significantly reduced when transplanted outside *F. serratus* range within the
472 rias, even when the outplant discs were placed beneath the canopies of other intertidal furoids, which feasibly
473 provided similar under-cover conditions as the target species. Indeed, the total canopy cover of furoids did not
474 differ between sites used for the transplant experiments. Adult canopies may reduce the survival of early post-
475 settlement stages by inducing whiplash and reducing the available light levels, but in the intertidal zone the
476 protection they offer from desiccation and heat stress during emersion periods probably outweighs the
477 negative effects (Vadas et al. 1992).

478 The performance of early developmental stages is probably more critical for *F. serratus* populations
479 than for other perennial fucoids, such as *F. vesiculosus* and *Ascophyllum nodosum*, which commonly form
480 mixed stands with the target species at mid-low intertidal levels of rias, while they spread downwards,
481 dominating at those levels in its absence (see results). The greater reliance on sexual reproduction is related to
482 the lack of capacity for vegetative regeneration of *Fucus serratus* (Malm et al. 2001), unlike the other two
483 species, which may resprout from their holdfasts (McCook & Chapman 1993, Åberg 1989). Demographic
484 models show a higher dependency on fertility for *Fucus serratus* populations than for the long-lived *A.*
485 *nodosum* (Åberg 1992a,b, Araújo et al. 2014).

486 Fucoids dominate a large part of intertidal rocky shores of rias. The total cover was negatively
487 correlated with wave action, in a pattern that is common in temperate coasts (Ballantine 1961). However,
488 wave forces did not emerge as a key factor in determining the confinement of *F. serratus* in rias, as significant
489 wave height was not found to be a relevant predictor in the species distribution model (SDM). Interestingly,
490 the distribution of *F. serratus* within rias closely matches that of *Himanthalia elongata*, despite the latter
491 being described as typical of more wave-exposed shores (Ballantine 1961). Indeed, *H. elongata* colonizes
492 more open shores than *F. serratus* and it remains more common at its southern range edge, in the NW Iberian
493 Peninsula (Martínez et al. 2012, Duarte et al. 2013).

494 Grazing is probably the most important biological factor controlling recruiting mortality in fucoids
495 (Chapman 1995), and it may limit the establishment of *F. serratus* towards the outer section of rias, where we
496 found the highest densities of grazing gastropods, most of which were epilithic microphagous species which
497 graze on early stages of macroalgae (Jones 1948, Lubchenco 1982, Crothers 2001). As already mentioned,
498 recruit survival is probably more critical for *F. serratus* populations than for other perennial fucoids, such as
499 *F. vesiculosus*, due to its lack of capacity for vegetative regeneration (Malm et al. 2001). Thus, wave action
500 could indirectly influence the distribution of the target species, by increasing the density of grazers, as shown
501 by Jonsson et al. (2006). Although we did not detect any differences in the growth of transplanted juveniles, in
502 the Ría de Muros they were substantially damaged by grazing when transplanted to outer locations, which also
503 supports the putative role of grazing pressure limiting the species distribution. The differences in grazing
504 habits and preferences of species may determine their primary control on either establishment (recruit
505 survival) or development (growth) of the fucoid. A few of the identified (such as the topshells *Littorina*

506 *obtusata*, Williams 1990), and other groups not considered here (small crustaceans and
507 herbivorous/omnivorous fishes), graze preferentially on fronds of established plants (Hawkins and Hartnoll
508 1983, Álvarez-Losada et al. 2020).

509 Consumer activity, however, could not explain the observed decline in survival of recruits towards the
510 innermost part of rias, where epilithic grazers were very scarce. Other factors such as sediment cover, salinity
511 and autumn water temperature may restrict the distribution towards the head of the rias. Accumulation of
512 substantial amounts of fine muddy sediments is common on rocky platforms at the sites close to the mouth of
513 rivers, generally located in the inner section of rias (except river Umia, see Fig. 1). Although the occurrence of
514 *F. serratus* was not linked to the presence/absence of sediment in the SDM, the abundance of deposits is
515 probably important. Models could thus be improved by incorporating a quantitative or semi-quantitative
516 variable of sediment load instead of a binary (presence/absence) parameter. Heavy sedimentation restricts
517 feeding activity and movements of epilithic grazers such as limpets (Airoldi & Hawkins 2007), and it directly
518 affects the settlement and survival of early post-settlement stages of seaweeds (Vadas et al. 1992), particularly
519 of *F. serratus* (Chapman et al. 2002).

520 Winter salinity and autumn seawater temperature were found to be important predictors in the SDM.
521 Low average salinity and decreased salinity during high precipitation events in winter may prevent
522 colonization by *F. serratus* at those sites most highly influenced by river discharges. Both fertilization success
523 and germination rates decreased substantially, with significant reductions in salinity, with *F. serratus* being
524 more sensitive than the congeneric *F. vesiculosus* to this type of environmental stress (Malm et al. 2001). Low
525 salinity appears to be the most important factor preventing the northward distribution of *F. serratus* in the
526 Baltic Sea (Malm et al. 2001). However, the species was frequent in rias at intermediate mean salinity, which
527 indicates the tolerance of these populations to moderate reductions. Recent experiments demonstrated that
528 survival of germlings from ria populations did not decrease when exposed for four weeks to a reduction in
529 average salinity from 35 to 22 ppt (García et al. 2021). It is not yet known whether this tolerance has a genetic
530 basis, as already detected in populations in a Norwegian fjord (Coyer et al. 2011). On the other hand, the
531 lower occurrence of *F. serratus* at sites with the highest salinity levels (more oceanic influence) could either
532 be a causal relationship or the result of co-varying factors, such as the increasing in grazing pressure towards

533 the outer section of rias, the influence of autumn seawater temperature (discussed below) and the overall
534 exclusion of furoids from the most exposed shores.

535 The autumn season is seldom considered in studies of climate change impacts, despite its importance
536 in the phenology (Brown et al. 2016, Gallinat et al. 2015) and geographic distributions of many species. This
537 gap in knowledge may be critical in the marine environment (Brown et al. 2016). Thus, winter and/or summer
538 sea temperatures have been described as determinants of the range boundaries of North Atlantic macroalgal
539 species, by limiting successful establishment or by lethal effects (Breeman 1988, Lüning 1990). Accordingly,
540 summer and winter are the only seasons typically considered when building SDMs for these key species of
541 temperate shores (e.g. Jueterbock et al. 2013, Assis et al. 2017). Although the results of our correlative SDM
542 do not necessarily involve causality (as mentioned above), there are reasons to support the role of autumn sea
543 temperature in determining the pattern of *F. serratus* occurrence inside the rias. Recruitment was observed
544 throughout the year, with May to September identified as the most favorable period (Duarte & Viejo 2018).
545 Following a summer with relatively benign conditions, characterized by cool and nutrient-rich waters
546 sustained by upwelling events (Fraga 1981), higher autumn temperatures might be critical for the success of
547 settlers in their transition to macroscopic stages. During autumn and winter, prevailing winds facilitate the
548 intrusion of warmer and more saline surface waters into the rias (Iglesias et al. 2008), being temperature
549 warmer than on the western coast of N Spain (Duarte & Viejo 2018). High temperatures affect the
550 performance of the early stages of *F. serratus* (Arrontes 1993), either individually or in combination with heat
551 stress during emersion (García et al. 2021). Temperature may play a more important role in shaping the fine-
552 grain distribution of *F. serratus* within rias than for *F. vesiculosus* and *A. nodosum*, given its low thermal
553 tolerance (Lüning 1984).

554 Our findings highlight the importance of several biotic and abiotic post-settlement filters in
555 determining the restricted distribution of *F. serratus* within rias, and they also suggest shifts in the important
556 factors acting along the rias (i.e. inner *versus* outer areas). Competition with other furoids, particularly with *F.*
557 *vesiculosus*, was previously proposed to be one of the drivers of the species distribution in the Rías Baixas
558 (Pazó & Niell 1977), but this was not tested experimentally in the present study. Rocky shore assemblages,
559 such as those in rias still dominated by canopy algae, are crowded systems where space is a common limited
560 resource, and therefore colonization processes should involve competitive displacements. This phenomenon

561 was observed during a short period of spread of *F. serratus* in N Spain, which was related to the decline of *F.*
562 *vesiculosus* (Arrontes 2002). The predominance of *F. serratus* over *F. vesiculosus* was also observed in a
563 long-term survey of experimentally cleared plots in British shores (Jenkins et al. 2004). The higher fecundity
564 of *F. serratus*, producing twice as many eggs as the congeneric species (Chapman 1995 and references
565 therein), along with the faster growth of young plants (Arrontes 2002), may explain this outcome.
566 Nevertheless, the opposite result, i.e. a clear predominance of *F. vesiculosus* over *F. serratus*, was detected in
567 field and laboratory experiments involving germlings and adult plants by Karez & Chapman (1998) and Karez
568 (2003). In this case the field experiments were conducted on the Island of Helgoland in the North Sea. The
569 outcome of competition is known to depend on the abiotic environmental conditions (Davis et al. 1998). The
570 spatial differences in habitat suitability for *F. serratus* within the rias may thus modulate competition,
571 precluding the species from thriving at those sites with other well-established canopy-forming species, while
572 preventing the downward spread of other fucoids on the shore, particularly *F. vesiculosus*, at those sites
573 favourable for the target species.

574 *F. serratus* exhibits low gamete dispersal, and its thalli lack floating vesicles, which limits its chances
575 of long-range colonization (as demonstrated by Arrontes 1993, 2002). The species was nonetheless able to
576 rapidly invade proximate sites during the range expansion occurring in N Spain around 1985-2000 (Arrontes
577 2002), and the probability of spread will probably increase in the semi-enclosed coastal waters of rias. We
578 thus hypothesize that habitat suitability is more crucial than dispersal constraints in determining the fine-grain
579 distribution of *F. serratus* within the rias, although further studies are needed for confirmation.

580 The restricted distribution of *F. serratus* within the rias appears so far relatively stable in time, lasting
581 since at least the 1960s (Ardre 1957, Donze, 1968, Pazó & Niell, 1977, this study). Further back in time,
582 Iberian shores acted as glacial refugium for *F. serratus* and other North Atlantic canopy-forming algae during
583 the Last Glacial Maximum (LGM), ~ 21 to 19.000 years before present (Coyer et al. 2003, Olsen et al. 2010,
584 Neiva et al. 2012). Recent paleo-oceanographic studies based on analysis of sediment cores from the western
585 Iberian margin indicated that sea surface temperature close to the coast was only slightly colder during the
586 LGM than in the Holocene (<8.000 years) and present times, although with some substantially colder periods
587 in between (Salgueiro et al. 2014). Remarkably, the western coast of the NW Iberian Peninsula appears to be a

588 climate refugium for large brown macroalgae during LGM, but also through the Holocene, nowadays still
589 providing benign conditions in an increasingly harsh regional context.

590 However, our model projections suggested the future extinction of *F. serratus* in these potential
591 refugia within western rias, with an increase of 1.5°C in maximum autumn temperature. Climate projections
592 for the western Iberian Peninsula suggest a buffering effect of the upwelling, resulting in less pronounced
593 warming along the coast than in the adjacent ocean (Varela et al. 2022). This is consistent with the observed
594 trends in all the eastern boundary upwelling systems over the past few decades (Seabra et al. 2019). In fact, a
595 greater buffering effect is expected in the NW Iberian Peninsula than in the rest of the upwelling system,
596 which suggests a northwards displacement of the Canary upwelling. Even with this buffering effect, an
597 average warming of 2° C is estimated for this upwelling area by the end of the century, relative to the
598 historical period (1970-1999), under the SSP5-8.5 greenhouse emission scenario (Varela et al. 2022). Further
599 within the Rías Baixas, ocean warming may be even higher, and the increase in water temperature could
600 exceed 2.5 ° C during summer months by the end of the century, relative to the historical period (Des et al.
601 2022).

602 The potential future extinction of *F. serratus* would trigger a reorganization of intertidal assemblages
603 in rias, with changes in the dominance of canopy species, similarly to what happened in Canadian shores
604 coinciding with sea warming events (Ugarte et al. 2009). If future conditions become more stressful, more
605 drastic changes would occur, with the complete loss of canopies and a shift to less complex and productive
606 turf-forming assemblages. Such shifts, leading to functionally impoverished coastal ecosystems, have already
607 been observed in many coastal areas worldwide, particularly in N Spain (Strain et al. 2014, Álvarez-Losada et
608 al. 2020). The impacts of warming can be further mediated or exacerbated by increased grazing pressure from
609 gastropods (Hawkins et al. 2008) and fishes, whose activity is increasing in temperate shores, affecting
610 subtidal kelps (Franco et al. 2015, Barrientos et al. 2022) as well as intertidal furoids (e.g. Álvarez-Losada et
611 al. 2020).

612 Both our model projection and that of a previous one developed at much broader scale suggested the
613 extinction of *F. serratus* at the southern edge of its range (Jueterbock et al. 2013), although our fine-resolution
614 model may better capture the environmental variability experienced by the species at this range edge and thus
615 the relevant predictors acting there. None of these correlative models considers the outcome of biotic

616 interactions or the potential ability of populations to cope with new conditions through plasticity and
617 adaptation (King et al. 2018). Previous studies show inter-population differences in the thermal tolerance of *F.*
618 *serratus* in the NW Iberian Peninsula, which suggest acclimatization or local adaptation to heterogeneous
619 conditions, with greater thermal tolerance in populations developed under more stressful conditions (García et
620 al. 2021). Although it has been argued that the lower genetic diversity detected in southern populations may
621 limit their ability to evolve (Coyer et al. 2003, Pearson et al. 2009), there is still no detailed genetic
622 information on populations within rias, and thus their capacity to cope with future changes remains
623 unresolved. Furthermore, the rate and trajectory of climate change rely on human decisions at a global scale,
624 which will define the real scenario of greenhouse emissions.

625 Our results highlight the role of autumn temperatures in shaping the current distribution and future
626 prospect of *F. serratus* in rias. We hypothesize that this season is more important than previously assumed for
627 this and other cold-temperate seaweeds at their warm range edge. Autumn is already the season with the
628 highest rates of SST increase in the NW Iberian Peninsula (Barrientos et al. 2020). Warmer autumns may
629 prolong heat stress experienced by seaweeds, especially in the absence or under a weaker influence of summer
630 upwelling events, leading to increased shedding of fronds and mortality. A clear increase in the mortality of
631 large adult plants of *F. serratus* was detected in autumn during the decline of marginal populations in N Spain
632 (unpublished data). Deterioration of adult plants would affect their reproductive output. Shortened
633 reproductive periods and more variable and reduced reproductive output have been documented in marginal
634 populations of *F. serratus* in N Spain and *F. guiryi* in Portugal (Viejo et al. 2011, Zardi et al. 2015, Duarte &
635 Viejo, 2018). With a narrower window of reproduction, commonly concentrated in spring-summer, the
636 success of settlers during autumn will become critical for persistence, particularly for species with a lifespan
637 of a few years, such as *Fucus* spp. The germling success may, in turn, be affected by the deterioration of adult
638 canopies, which would reduce the protection that the canopies provide from desiccation and heat stress during
639 emersion. More than one critical effect of temperature may restrict species distribution, with impacts at one
640 life stage added to or amplified by the effects at other phases (Breeman 1988). Moreover, the responses of
641 large brown seaweeds to heat stress may be triggered by extreme events but also by cumulative, prolonged
642 warming conditions below extreme values (Straub et al. 2022).

643

644 **Acknowledgements**

645 We are particularly grateful to Linney Duarte for collaboration in the fieldwork. We also thank the staff at the
646 Instituto Tecnológico para o Control do Medio Mariño de Galicia (Inctemar, Xunta de Galicia, Vilagarcía de
647 Arousa, Spain) for providing dissolved inorganic nutrients values for stations in the rias under study. We are
648 very grateful to three anonymous reviewers for their insightful comments and suggestions, and we also thank
649 to Christine Francis for linguistic assistance. Funding was provided by the Spanish Ministry of Science and
650 Innovation (projects CGL2010-1931 and CGL2014-60193-P) and by the Autonomous Government, Xunta de
651 Galicia, ERDF under projects ED431C 2021/44-GRC and ED431C 2021/42 (Grupos de Referencia
652 Competitiva): ‘ERDF A way of making Europe’. M.D. was supported by the Xunta de Galicia through a
653 postdoctoral grant ED481B-2021-103.

654

655 **Literature Cited**

- 656 Åberg P (1989) Distinguishing between genetic individuals in *Ascophyllum nodosum* populations on the
657 Swedish West Coast. *Br Phycol J* 24:183-190
- 658 Åberg P (1990) Measuring size and choosing category size for a transition matrix study of the seaweed
659 *Ascophyllum nodosum*. *Mar Ecol Prog Ser* 63: 281-287
- 660 Åberg P (1992a) A demographic study of two populations of the seaweed *Ascophyllum nodosum*. *Ecology* 73:
661 1488-1501
- 662 Åberg P (1992b) Size-based demography of the seaweed *Ascophyllum nodosum* in stochastic environments.
663 *Ecology* 73: 1473-1487
- 664 Airoidi L, Hawkins SJ (2007) Negative effects of sediment deposition on grazing activity and survival of the
665 limpet *Patella vulgata*. *Mar Ecol Prog Ser* 332: 235-240
- 666 Álvarez-Losada Ó, Arrontes J, Martínez B, Fernández C, Viejo RM (2020) A regime shift in intertidal
667 assemblages triggered by loss of algal canopies: A multidecadal survey. *Mar Environ Res* 160:104981
668 <https://doi.org/10.1016/j.marenvres.2020.104981>
- 669 Araújo RM, Serrão EA, Sousa-Pinto I, Åberg P (2014) Spatial and temporal dynamics of furoid populations
670 (*Ascophyllum nodosum* and *Fucus serratus*): A comparison between central and range edge populations.
671 *PLoS One* 9: e92117. <https://doi.org/10.1371/journal.pone.0092177>
- 672 André F (1957) Florule hivernale de la Ría de Vigo. *Rev Algologique* 3:135-146
- 673 Arrontes J (1993) Nature of the distributional boundary of *Fucus serratus* on the North shore of Spain. *Mar*
674 *Ecol Prog Ser* 93: 183-193

- 675 Arrontes J (2002) Mechanisms of range expansion in the intertidal brown alga *Fucus serratus* in northern
676 Spain. Mar Biol 141:1059–1067 <https://doi.org/10.1007/s00227-002-0910-x>
- 677 Ashcroft MB (2010). Identifying refugia from climate change. J Biogeogr 37: 1407–1413
678 <https://doi.org/10.1111/j.1365-2699.2010.02300.x>
- 679 Assis J, Berecibar E, Claro B, Alberto F, Reed D , Raimondi P, Serrão EA (2017) Major shifts at the range
680 edge of marine forests: The combined effects of climate changes and limited dispersal. Sci Rep 7: 44348
681 <https://doi.org/10.1038/srep44348>
- 682 Ballantine WJ (1961) A biologically defined exposure scale for the comparative description of rocky shores.
683 Field Stud 1: 1-19
- 684 Barrientos S, Barreiro R, Cremades J, Piñeiro-Corbeira C (2020) Setting the basis for a long-term monitoring
685 network of intertidal seaweed assemblages in northwest Spain. Mar Environ Res 160:105039
686 <https://doi.org/10.1016/j.marenvres.2020.105039>
- 687 Barrientos, S., Piñeiro-Corbeira C, Barreiro R (2022) Temperate Kelp Forest Collapse by Fish Herbivory: A
688 Detailed Demographic Study. Front Mar Sci 9: 817021 <https://doi.org/10.3389/fmars.2022.817021>
- 689 Barton K (2012) MuMIn: Multi-model inference. R package version 1.7.2. [https://cran.r-](https://cran.r-project.org/web/packages/MuMIn/)
690 [project.org/web/packages/MuMIn/](https://cran.r-project.org/web/packages/MuMIn/)
- 691 Botas JA, Fernández E, Bode A, Anadón R (1990) A persistent upwelling off the Central Cantabrian Coast
692 (Bay of Biscay). Estuar Coast Shelf Sci 30:185–189
- 693 Breeman AM (1988) Relative importance of temperature and other factors in determining geographic
694 boundaries of seaweeds: experimental and phenological evidence. Helgol Meeresunters 42: I99-241
- 695 Brown CJ, O'Connor MI, Poloczanska ES, Schoeman DS, Buckley LB, Burrows MT, Duarte CM, Halpern
696 BS, Pandolfi JM, Parmesan C, Richardson AJ (2016) Ecological and methodological drivers of species'
697 distribution and phenology responses to climate change. Glob Change Biol 22:1548–1560
698 <https://doi.org/10.1111/gcb.13184>
- 699 Brown JH (1984). On the relationship between abundance and distribution of species. Am Nat 124:255-279
- 700 Bruelheide H, Scheidel U (1999). Slug herbivory as a limiting factor for the geographical range of *Arnica*
701 *montana*. J Ecol 87:839–848
- 702 Casado-Amezúa P, Araújo R, Bárbara I, Bermejo R, Borja Á, Díez I, Fernández C, Gorostiaga JM, Guinda X,
703 Hernández I, Juanes JA, Peña V, Peteiro C, Puente A, Quintana I, Tuya F, Viejo RM, Altamirano M,
704 Gallardo T, Martínez B (2019). Distributional shifts of canopy-forming seaweeds from the Atlantic coast
705 of Southern Europe. Biodiver Conserv 28: 1151-1172 <https://doi.org/10.1007/s10531-019-01716-9>.
- 706 Case TJ, Holt RD, McPeck MA, Keitt TH (2005) The community context of species' borders: ecological and
707 evolutionary perspectives. Oikos 108: 28-46
- 708 Chapman ARO (1995) Functional ecology of furoid algae: twenty-three years of progress. Phycologia 34: 1-
709 32
- 710 Chapman AS, Albrecht AS, Fletcher RL (2002) Differential effects of sediments on survival and growth of
711 *Fucus serratus* embryos (Fucales, Phaeophyceae). J Phycol 38: 894-903

- 712 Coyer JA, Peters AF, Stam WT, Olsen JL (2003) Post-ice age recolonization and differentiation of *Fucus*
713 *serratus* L. (Phaeophyceae; Fucaceae) populations in Northern Europe. Mol Ecol 12:1817–1829
714 <https://doi.org/10.1046/j.1365-294X.2003.01850.x>
- 715 Coyer JA, Hoarau G, Pearson G, Mota C, Jüterbock A, Alpermann T, John U, Olsen JL (2011) Genomic
716 scans detect signatures of selection along a salinity gradient in populations of the intertidal seaweed
717 *Fucus serratus* on a 12km scale. Mar Genomics 4:41–49 <https://doi.org/10.1016/j.margen.2010.12.003>
- 718 Crothers JH (2001) Common topshells: an introduction to the biology of *Osilinus lineatus* with notes on other
719 species in the genus. Field Stud 10: 115-160
- 720 Dallas TA, Santini L, Decker R, Hastings A (2020) Weighing the evidence for the abundant-center
721 hypothesis. Biodivers Inform 15:81-91 <https://doi.org/10.17161/bi.v15i3.11989>
- 722 Davis AJ, Jenkinson LS, Lawton JH, Shorrocks B, Wood S (1998) Making mistakes when predicting shifts in
723 species range in response to global warming. Nature 391: 783-786
- 724 Des M, deCastro M, Sousa MC, Dias JM, Gómez-Gesteira M (2019). Hydrodynamics of river plume intrusion
725 into an adjacent estuary: the Minho River and Ria de Vigo. J Mar Syst 189: 87–97
726 <https://doi.org/10.1016/j.jmarsys.2018.10.003>.
- 727 Des M, Gómez-Gesteira M, deCastro M, Gómez-Gesteira L, Sousa MC (2020). How can ocean warming at
728 the NW Iberian Peninsula affect mussel aquaculture? Sci Total Environ 709: 136117
729 <https://doi.org/10.1016/j.scitotenv.2019.136117>.
- 730 Des M, Gómez-Gesteira JL, deCastro M, Iglesias D, Sousa MC, ElSerafy G, Gómez-Gesteria M (2022).
731 Historical and future naturalization of *Magallana gigas* in the Galician coast in a context of climate
732 change. Sci Total Environ 838: 156437 <https://doi.org/10.1016/j.scitotenv.2022.156437>
- 733 Diniz-Filho JAF, Rangel TFLVB, Bini LM (2008) Model selection and information theory in geographical
734 ecology. Glob Ecol Biogeogr 17: 479–488
- 735 Donze M (1968) The algal vegetation of the Ría de Arousa (NW, Spain). Blumea 16: 159-192
- 736 Dormann CF, Elith J, Bacher S, Buchmann C, Carl G, Carré G, García-Márquez JR, Gruber B, Lfourcade B,
737 Leitão PJ, Münkemüller T, McClean C, Osborne PE, Reineking B, Schröder B, Skidmore AK, Zurell D,
738 Lautenbach S (2013) Collinearity: A review of methods to deal with it and a simulation study evaluating
739 their performance. Ecography 36:27–46 <https://doi.org/10.1111/j.1600-0587.2012.07348.x>
- 740 Duarte L, Viejo RM (2018) Environmental and phenotypic heterogeneity of populations at the trailing range-
741 edge of the habitat-forming macroalga *Fucus serratus*. Mar Environ Res 136:16–26
742 <https://doi.org/10.1016/j.marenvres.2018.02.004>
- 743 Duarte L, Viejo RM, Martínez B, deCastro M, Gómez-Gesteira M, Gallardo T (2013) Recent and historical
744 range shifts of two canopy-forming seaweeds in North Spain and the link with trends in sea surface
745 temperature. Acta Oecol 51:1–10 <https://doi.org/10.1016/j.actao.2013.05.002>
- 746 Fernández C (2016) Current status and multidecadal biogeographical changes in rocky intertidal algal
747 assemblages: The northern Spanish coast. Estuar Coast Shelf Sci 171:35–40
748 <https://doi.org/10.1016/j.ecss.2016.01.026>

- 749 Fielding AH, Bell JF (1997) A review of methods for the assessment of prediction errors in conservation
750 presence/absence models. *Environ Conserv* 24: 38-49
- 751 Fischer-Piette E (1955) Sur les déplacements des frontières biogéographiques intercotidales, observables en
752 Espagne: situation en 1954-1955. *C R Seances Acad Sci* 241: 447-449
- 753 Fraga F (1981) Upwelling off the Galician coast, northwest Spain. *Coast Estuar Sci* 1:176-182
- 754 Franco JN, Wernberg T, Bertocci I, Duarte P, Jacinto D, Vasco-Rodrigues N, Tuya F (2015) Herbivory drives
755 kelp recruits into “hiding” in a warm ocean climate. *Mar Ecol Prog Ser* 536:1–9
756 <https://doi.org/10.3354/meps11445>
- 757 Gaston KJ (2003) The structure and dynamics of geographic ranges. Oxford University Press. Oxford, UK
- 758 Gallinat AS, Primack RB, Wagner DL (2015) Autumn, the neglected season in climate change research.
759 *Trends Ecol Evol* 30:169–176
- 760 García AG, Olabarria C, Álvarez-Losada Ó, Viejo RM (2021) Differential responses of trailing-edge
761 populations of a foundation alga to thermal stress. *Eur J Phycol* 56: 373-388
762 <https://doi.org/10.1080/09670262.2020.1842909>
- 763 Gillingham PK, Huntley B, Kunin WE, Thomas CD (2012) The effect of spatial resolution on projected
764 responses to climate warming. *Divers Distrib* 18:990–1000 <https://doi.org/10.1111/j.1472-4642.2012.00933.x>
765
- 766 Gilman SE (2006) Life at the edge: an experimental study of a poleward range boundary. *Oecologia* 148:270–
767 279
- 768 Greiser C, Hylander K, Meineri E, Luoto M, Ehrlén J (2020) Climate limitation at the cold edge: contrasting
769 perspectives from species distribution modelling and a transplant experiment. *Ecography* 43: 637–647
770 <https://doi.org/10.1111/ecog.04490>
- 771 Guisan A, Zimmermann NE (2000) Predictive habitat distribution models in ecology. *Ecol Modell* 135:147–
772 186
- 773 Hampe A, Petit RJ (2005) Conserving biodiversity under climate change: The rear edge matters. *Ecol Lett*
774 8:461–467
- 775 Hannah L, Flint L, Syphard AD, Syphard AD, Moritz MA, Buckley LB, McCullough IM (2014) Fine-grain
776 modeling of species’ response to climate change: oldouts, stepping-stones, and microrefugia. *Trends*
777 *Ecol Evol* 29:390–397
- 778 Hargreaves AL, Samis KE, Eckert CG. (2014). Are Species’ Range Limits Simply Niche Limits Writ Large?
779 A Review of Transplant Experiments beyond the Range. *Am Nat* 183: 157-173
780 <https://doi.org/10.1086/674525>
- 781 Hawkins SJ, Hartnoll RG (1983). Grazing of intertidal algae by marine invertebrates. *Oceanogr Mar Biol*
782 *Annu Rev* 21:195-282
- 783 Hawkins SJ, Moore PJ, Burrows MT, Poloczanska E, Mieszkowska N, Herbert RJH, Jenkins SR, Thompson
784 RC, Genner MJ, Southward AJ (2008) Complex interactions in a rapidly changing world: Responses of
785 rocky shore communities to recent climate change. *Clim Res* 37: 123–133

- 786 Holt RD, Keitt TH (2005). Species' borders: a unifying theme in ecology. *Oikos* 108:3-6
- 787 Iglesias G, Carballo R, Castro A (2008) Baroclinic modelling and analysis of tide- and wind-induced
788 circulation in the Ría de Muros (NW Spain). *J Mar Syst* 74:475–484
789 <https://doi.org/10.1016/j.jmarsys.2008.03.009>
- 790 Jenkins SR, Norton TA, Hawkins SJ (2004). Long term effects of *Ascophyllum nodosum* canopy removal on
791 mid shore community structure. *J Mar Biolog Assoc UK* 84: 327–329
792 <https://doi.org/10.1017/S0025315404009221h>.
- 793 Jones NS (1948) Observations and experiments on the biology of *Patella vulgata* at Port St. Mary, Isle of
794 Man. *Proc Trans Liverpool Biol Soc* 56: 60-77
- 795 Jonsson PR, Granhag L, Moschella PS, Aberg P, Hawkins SJ, Thompson RC (2006) Interactions between
796 wave action and grazing control the distribution of intertidal macroalgae. *Ecology* 87:1169-1178
- 797 Jueterbock A, Tyberghein L, Verbruggen H, Coyer JA, Olsen JL, Hoarau G (2013) Climate change impact on
798 seaweed meadow distribution in the North Atlantic rocky intertidal. *Ecol Evol* 3:1356–1373
799 <https://doi.org/10.1002/ece3.541>
- 800 Kämpf J, Chapman P (2016) The Canary/Iberia Current Upwelling System. In: *Upwelling Systems of the*
801 *World*. Springer International Publishing, pp 203–250
- 802 Karez R (2003) Competitive ranks of three *Fucus* spp. (Phaeophyta) in laboratory experiment - Testing of
803 Keddy's competitive hierarchy model. *Helgol Mar Res* 57:83–90 [https://doi.org/10.1007/s10152-003-](https://doi.org/10.1007/s10152-003-0136-4)
804 [0136-4](https://doi.org/10.1007/s10152-003-0136-4)
- 805 Karez R, Chapman ARO (1998) A Competitive Hierarchy Model Integrating Roles of Physiological
806 Competence and Competitive Ability Does Not Provide a Mechanistic Explanation for the Zonation of
807 Three Intertidal *Fucus* Species in Europe. *Oikos* 81: 471-494
- 808 King NG, McKeown NJ, Smale DA, Moore PJ (2018) The importance of phenotypic plasticity and local
809 adaptation in driving intraspecific variability in thermal niches of marine macrophytes. *Ecography*
810 41:1469–1484
- 811 Knight, M. and Parke, M. 1950. A biological study of *Fucus vesiculosus* and *Fucus serratus*. *J Mar Biolog*
812 *Assoc UK* 26: 439-515
- 813 Kusuma DW, Murdimanto A, Sukresno B, Jatisworo D, Hanintyo DR (2018) Comparison of interpolation
814 methods for sea surface temperature data. *J Fish Mar Sci* 2: 103-115
815 <https://doi.org/10.21776/ub.jfmr.2018.002.02.7>
- 816 Landis JR & Kock GG (1977) The Measurement of Observer Agreement for Categorical Data. *Biometrics* 33:
817 159-174
- 818 Lee-Yaw JA, Kharouba HM, Bontrager M, Mahony C, Csergő AM, Noreen AME, Li Q, Schuster R, Angert
819 AL (2016) A synthesis of transplant experiments and ecological niche models suggests that range limits
820 are often niche limits. *Ecol Lett* 19: 710–722
- 821 Lembrechts JJ, Nijs I, Lenoir J (2019) Incorporating microclimate into species distribution models. *Ecography*
822 42:1267–1279

- 823 Lennon JJ, Kunin WE, Corne S, Carver S, Van Hees WW (2002) Are Alaskan trees found in locally more
824 favourable sites in marginal areas? *Glob Ecol Biogeogr* 11(2): 103-114.
- 825 Lubchenco J (1982) Effects of grazers and algal competitors on furoid colonization in tide pools. *J Phycol*
826 18:544–550 <https://doi.org/10.1111/j.1529-8817.1982.tb03221.x>
- 827 Lüning K (1984) Temperature tolerance and biogeography of seaweeds: the marine algal flora of Helgoland
828 (North Sea) as an example. *Helgol Meeresunters* 38: 305-317
- 829 Lüning K (1990) *Seaweeds: Their environment, biogeography and ecophysiology*. Wiley-Interscience, New
830 York.
- 831 MacArthur RH (1972) *Geographical ecology: patterns in the distribution of species*. Harper and Row, New
832 York.
- 833 Maggs CA, Castilho R, Foltz D, Henzler C, Jolly MT, Kelly J, Olsen J, Perez KE, Stam W, Väinölä R, Viard
834 F, Wares J. (2008) Evaluating signatures of glacial refugia for North Atlantic benthic marine taxa.
835 *Ecology* 89: S108–S122 <https://doi.org/10.1890/08-0257.1>
- 836 Malm T, Kautsky L, Engkvist R (2001) Reproduction, recruitment and geographical Distribution of *Fucus*
837 *serratus* L. in the Baltic Sea. *Bot Mar* 44:101-108
- 838 Martin PH, Canham CD (2020) Peaks in frequency, but not relative abundance, occur in the center of tree
839 species distributions on climate gradients. *Ecosphere* 11:e03149. <https://doi.org/10.1002/ecs2.3149>
- 840 Martínez B, Viejo RM, Carreño F, Aranda SC (2012) Habitat distribution models for intertidal seaweeds:
841 Responses to climatic and non-climatic drivers. *J Biogeogr* 39:1877–1890
842 <https://doi.org/10.1111/j.1365-2699.2012.02741.x>
- 843 McCook LJ, Chapman ARO (1991). Community succession following massive ice-scour on an exposed rocky
844 shore: effects of *Fucus* canopy algae and of mussels during late succession. *J Exp Mar Biol Ecol* 154:
845 137- 169
- 846 Miranda F (1934) Materiales para una flora marina de las Rías Bajas Gallegas. *Bol R Soc Esp Hist Nat* 34:
847 165-180
- 848 Muguerza N, Arriaga O, Díez I, Becerro MA, Quintano E, Gorostiaga JM (2022) A spatially-modelled
849 snapshot of future marine macroalgal assemblages in southern Europe: Towards a broader
850 Mediterranean region? *Mar Environ Res* 176:105592 <https://doi.org/10.1016/j.marenvres.2022.105592>
- 851 Neiva J, Pearson GA, Valero M, Serrão EA (2012) Drifting fronds and drifting alleles: Range dynamics, local
852 dispersal and habitat isolation shape the population structure of the estuarine seaweed *Fucus ceranoides*.
853 *J Biogeogr* 39:1167–1178 <https://doi.org/10.1111/j.1365-2699.2011.02670.x>
- 854 Oldfather MF, Kling MM, Sheth SN, et al (2020) Range edges in heterogeneous landscapes: Integrating
855 geographic scale and climate complexity into range dynamics. *Glob Chang Biol* 26:1055–1067
856 <https://doi.org/10.1111/gcb.14897>
- 857 Oliver T, Hill JK, Thomas CD, Brereton T, Roy DB (2009). Changes in habitat specificity of species at their
858 climatic range boundaries. *Ecol Lett* 12: 1091–1102 <https://doi.org/10.1111/j.1461-0248.2009.01367.x>

- 859 Olsen JL, Zechman FW, Hoarau G, Coyer JA, Stam WT, Valero M, Åberg P (2010) The phylogeographic
860 architecture of the furoid seaweed *Ascophyllum nodosum*: An intertidal “marine tree” and survivor of
861 more than one glacial-interglacial cycle. *J Biogeogr* 37:842–856 [https://doi.org/10.1111/j.1365-](https://doi.org/10.1111/j.1365-2699.2009.02262.x)
862 [2699.2009.02262.x](https://doi.org/10.1111/j.1365-2699.2009.02262.x)
- 863 Otero P, Ruiz-Villarreal M, Peliz Á, Cabanas JM (2010) Climatología y reconstrucción de series temporales
864 de descarga fluvial en el Noroeste de Iberia: Influencia en el balance de densidad sobre la plataforma.
865 *Sci Mar* 74:247–266 <https://doi.org/10.3989/scimar.2010.74n2247>
- 866 Pazó JP, Niell FX (1977) Distribución y características de *Fucus serratus* L. en las Rías Bajas Gallegas.
867 *Investig Pesq* 41:455–472
- 868 Pearson RG, Dawson TE (2003) Predicting the impacts of climate change on the distribution of species: are
869 bioclimate envelope models useful? *Glob Ecol and Biogeogr* 12: 361–371
- 870 Pearson GA, Lago-Leston A, Mota C (2009) Frayed at the edges: Selective pressure and adaptive response to
871 abiotic stressors are mismatched in low diversity edge populations. *J Ecol* 97:450–462
872 <https://doi.org/10.1111/j.1365-2745.2009.01481.x>
- 873 Richards S.A., Whittingham M.J., Stephens P.A. (2011) Model selection and model averaging in behavioural
874 ecology: the utility of the IT-AIC framework. *Behav Ecol Sociobiol* 65:77-89
- 875 R Development Core Team (2014). R: A language and environment for statistical computing. R Foundation
876 for Statistical Computing, Vienna, Austria.
- 877 Robin X, Turck N, Hainard A, Tiberti N, Lisacek F, Sanchez J, Müller M (2011). pROC: an open-source
878 package for R and S+ to analyze and compare ROC curves. *BMC Bioinformatics* 12:77
- 879 Sagarin RD, Gaines SD, Gaylord B (2006) Moving beyond assumptions to understand abundance
880 distributions across the ranges of species. *Trends Ecol Evol* 21:524–530
- 881 Salgueiro E, Naughton F, Voelker AHL, et al (2014) Past circulation along the western Iberian margin: A time
882 slice vision from the Last Glacial to the Holocene. *Quat Sci Rev* 106:316–329
883 <https://doi.org/10.1016/j.quascirev.2014.09.001>
- 884 Sandrini-Neto L, Camargo MG (2014). GAD: an R package for ANOVA designs from general principles.
885 Available on CRAN. Vienna: R Foundation for Statistical Computing.
- 886 Schiel DR (2006) Rivets or bolts? When single species count in the function of temperate rocky reef
887 communities. *J Exp Mar Biol Ecol* 338:233–252 <https://doi.org/10.1016/j.jembe.2006.06.023>
- 888 Seabra R, Varela R, Santos AM, Gómez-Gesteira M, Meneghesso C, Whetey DS, Lima FP (2019) Reduced
889 nearshore warming associated with eastern boundary upwelling systems. *Front Mar Sci* 6:104
890 <https://doi.org/10.3389/fmars.2019.00104>
- 891 Sexton JP, McIntyre PJ, Angert AL, Rice KJ (2009) Evolution and ecology of species range limits. *Annu Rev*
892 *Ecol Evol Syst* 40:415–436. <https://doi.org/10.1146/annurev.ecolsys.110308.120317>
- 893 Stanton-Geddes, Tiffin P, Shaw RG (2012). Role of climate and competitors in limiting fitness across range
894 edges of an annual plant. *Ecology* 93: 1604–1613

- 895 Strain EMA, Thomson RJ, Micheli F, Mancuso FP, Airoidi L (2014) Identifying the interacting roles of
896 stressors in driving the global loss of canopy-forming to mat-forming algae in marine ecosystems. *Glob*
897 *Change Biol* 20:3300–3312 <https://doi.org/10.1111/gcb.12619>
- 898 Streiner DL and Carney J (2007). What's Under the ROC? An Introduction to Receiver Operating
899 Characteristics Curves. *Can J Psychiatry* 2007: 121–128
- 900 Straub SC, Wernberg T, Marzinelli EM, Vergés A, Kelaher BP, Coleman MA (2022) Persistence of seaweed
901 forests in the anthropocene will depend on warming and marine heatwave profiles. *J Phycol* 58:22–35.
902 <https://doi.org/10.1111/jpy.13222>
- 903 Ugarte RA, Critchley A, Serdynska AR, Deveau JP (2009) Changes in composition of rockweed
904 (*Ascophyllum nodosum*) beds due to possible recent increase in sea temperature in eastern Canada. *J*
905 *Appl Phycol* 21:591–598. <https://doi.org/10.1007/s10811-008-9397-2>
- 906 Vadas RL, Johnson JS, Norton TA (1992) Recruitment and mortality of early post-settlement stages of benthic
907 algae. *Br Phycol J* 27:331–351 <https://doi.org/10.1080/00071619200650291>
- 908 Vale CG, Tarroso P, Brito JC (2014) Predicting species distribution at range margins: Testing the effects of
909 study area extent, resolution and threshold selection in the Sahara-Sahel transition zone. *Divers Distrib*
910 20:20–33 <https://doi.org/10.1111/ddi.12115>
- 911 Varela R, Rodríguez-Díaz L, de Castro M, Gómez-Gesteira M (2022) Influence of Canary upwelling system
912 on coastal SST warming along the 21st century using CMIP6 GCMs. *Glob Planet Change* 208: 103692
913 <https://doi.org/10.1016/j.gloplacha.2021.103692>
- 914 Viejo RM, Martínez B, Arrontes J, Astudillo C, Hernández L (2011) Reproductive patterns in central and
915 marginal populations of a large brown seaweed: drastic changes at the southern range limit. *Ecography*
916 34: 75-84. <https://doi.org/10.1111/j.1600-0587.2010.06365.x>.
- 917 Willi Y, Van Buskirk J (2019) A Practical Guide to the Study of Distribution Limits. *Am Nat* 193: 773-785
- 918 Williams G.A (1990). The comparative ecologies of the flat periwinkles, *Littorina obstusata* (L.) and
919 *L.mariae* Sacchi et Rastelli. *Field Stu* 7: 469-482.
- 920 Zardi GI, Nicastro KR, Serrao EA, Jacinto R, Monteiro CA, Pearson GA (2015) Closer to the rear edge:
921 Ecology and genetic diversity down the core-edge gradient of a marine macroalga. *Ecosphere* 6:1-25
922 <https://doi.org/10.1890/ES14-00460.1>
- 923 Zuur A, Ieno EN, Walker N, Saveliev AA, Smith GM (2009) Mixed effects models and extensions in ecology
924 with R. Springer Science and Business Media.

925

926

927

928 Table 1. a) ANOVA for differences between rias (Muros, Arousa), between Locations (interior, origin,
 929 exterior) and Sites in the total cover of furoid species. Homogeneous variances; b) ANOVA for testing the
 930 effects of Date, Rias, Locations and Sites on the density of grazers. Variances were homogeneous after
 931 square-root data transformation. *A posteriori* SNK comparisons after significant Ria x Location interaction are
 932 also shown. E = Exterior, I = interior, O = Origin locations.

a) Total cover of furoids				
Source	df	MS	F	p
Ria, Ri	1	5165.964	4.330	0.083
Location, Lo	2	2789.971	2.338	0.177
Ri x Lo	2	1412.471	1.184	0.369
Site (Ri x Lo)	12	1193.119	5.783	<0.001
Residual	53 ⁽¹⁾	206.308		
b) Density of macrograzers				
Source	df	MS	F	p
Date, D	1	4.110	1.76	0.209
Ria, Ri	1	0.946	0.64	0.440
Location, Lo	2	118.321	79.64	<0.001
D x Ri	1	0.710	0.30	0.591
D x Lo	2	0.845	0.36	0.704
Ri x Lo	2	27.785	18.70	<0.001
D x Ri x Lo	2	5.195	2.22	0.151
Site (Ri x Lo)	12	1.486	2.45	0.007
D x Site (Ri x Lo)	12	2.336	3.85	<0.001
Residual	108	0.606		
SNK test Ri x Lo				
	Arousa	Muros		
E vs O	p<0.05	p < 0.001		
O vs I	ns	p < 0.001		
E vs I	p < 0.01	p< 0.001		

950

951 (1) One value was replaced by the mean of the correspondent site, and 1 df subtracted from the
 952 residual

953

954 Table 2. a) Likelihood ratio test (LRT) for GLMs testing differences in germling survival between rias (Ri:
 955 Arousa, Muros) and locations (Lo: origin, exterior and interior). The full model (M₁) was simplified by
 956 removing the interaction term Ri x Lo; b) Parameter estimates (fitted values) and standard errors (SE) of the
 957 simplified model (M₂). The fitted value for the origin location in Ría de Arousa was considered the reference
 958 level, and the other estimates are differences from this level. Dispersion parameter of M₂=1.40.

959

960

a) Model	Theta parameter	df	2loglik	Δdf	LRT	p
M ₁ , Full (Ri+Lo+ Ri x Lo)	0.571	59	-417.842			
M ₂ (-Ri x Lo)	0.630	57	-412.668	2	5.174	0.075

b) Parameters	Estimate	SE	Z-value	p
Ri:Arousa, Lo:Origin	2.774	0.328	8.463	<0.001
Ri: Muros	0.493	0.349	1.415	0.157
Lo:Exterior	-1.154	0.431	-2.675	0.007
Lo:Interior	-1.015	0.410	-2.475	0.013

972

973

974

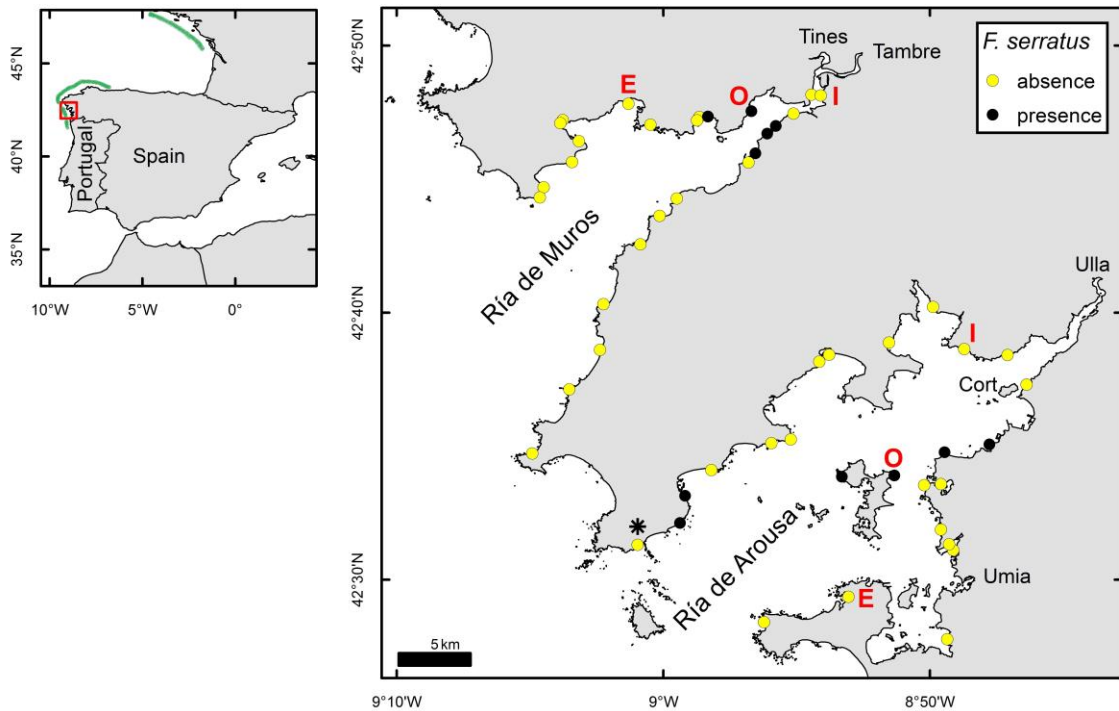
975

Table 3. a) Summary of the best model for *F. serratus* occurrence within rias. T-Aut: maximum sea temperature in autumn; Sal: mean salinity in January-February (quadratic component included, Sal²); Expl. Dev.: Explained Deviance. Values in parenthesis are the standard errors of parameters; b) Performance metrics of the model, calibrated on jackknife scores: relative true presences (sensitivity, RTP); relative true absences or specificity (RTA); the kappa coefficient (k); and the area under the receiver operating characteristic curve (AUC). The prevalence rate was 0.22.

a)					
Intercept	T –Aut	Sal	Sal ²	AIC	Expl. Dev. (%)
-8920.00	-28.48	553.47	-8.15	29.30	59.95
(3613.62)	(11.75)	(222.71)	(3.28)		
b)					
RTP	RTA	k	AUC		
0.73	0.80	0.45 ^a	0.907 ^b		

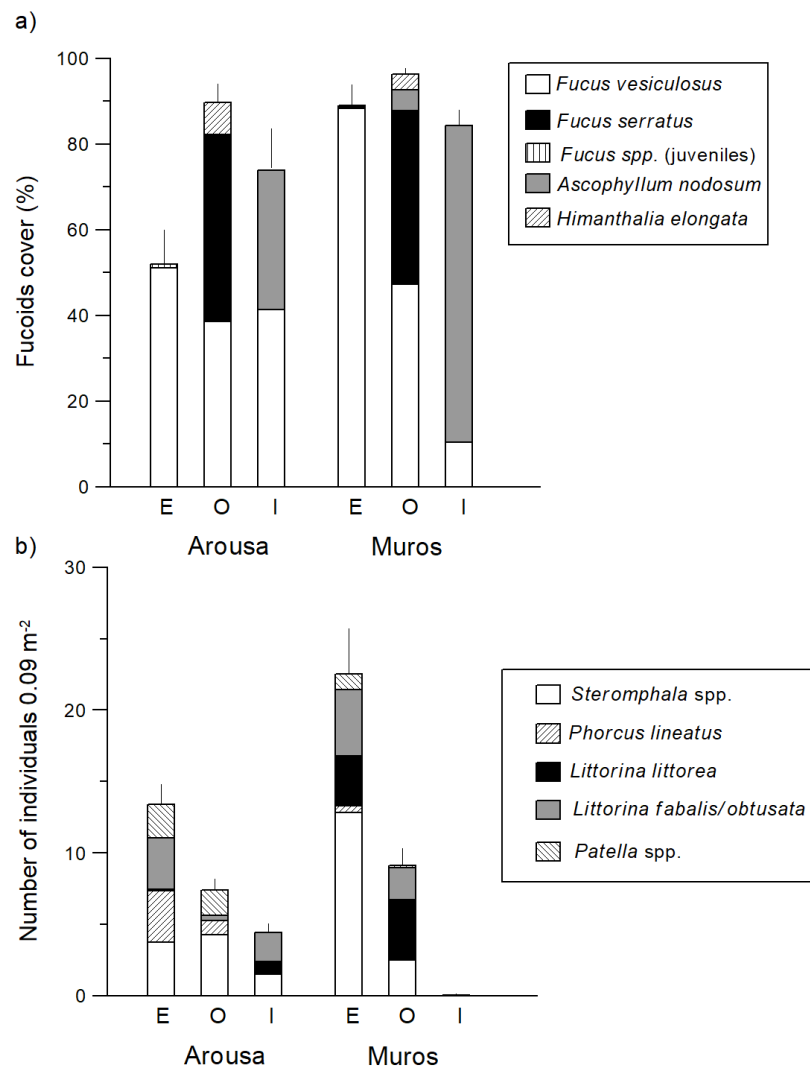
^a good, according to Landis & Kock 1977

^bhigh accuracy, according to Streiner and Cairney (2007)

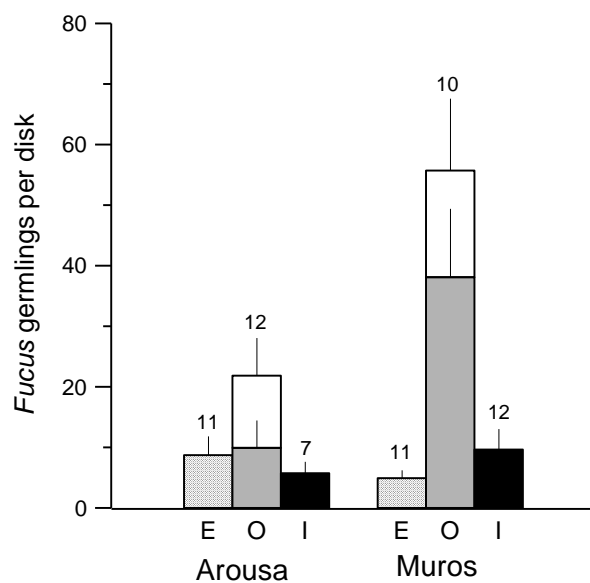


979

980 Figure 1. Study area (green band shows the distribution of *Fucus serratus*) and surveyed locations of rias with
 981 presence (black circles) and absence (yellow circles) of *F. serratus* (2011-2013 sampling). Letters show the
 982 exterior (E), origin (O) and interior (I) locations where transplant experiments were carried out. Cort: Isla de
 983 Cortegada. Mouth of rivers Tines and Tambre (Ría de Muros) and Ulla and Umia (Ría de Arousa) are also
 984 indicated. The asterisk marks the Río Azor site, where the species is currently absent (see text).



985 Figure 2. a) Total fucoid cover in origin (O), exterior (E) and interior (I) locations of the transplant
 986 experiments in Rías of Arousa and Muros, in May 2012; b) Density of macrograzers in the studied locations
 987 (data of May and July 2012 were pooled). Means \pm SE are shown, n = 12 in (a), n = 24 in (b), number per
 988 location.

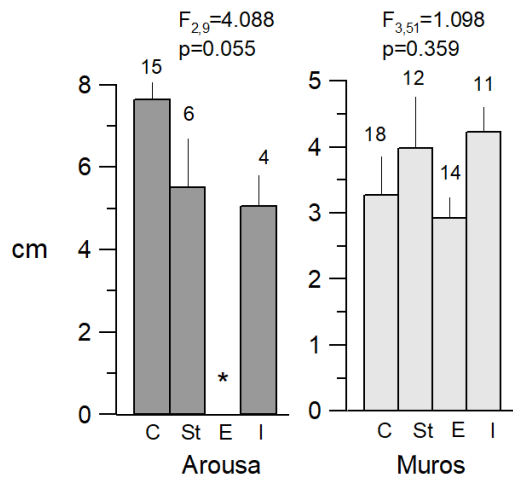


989

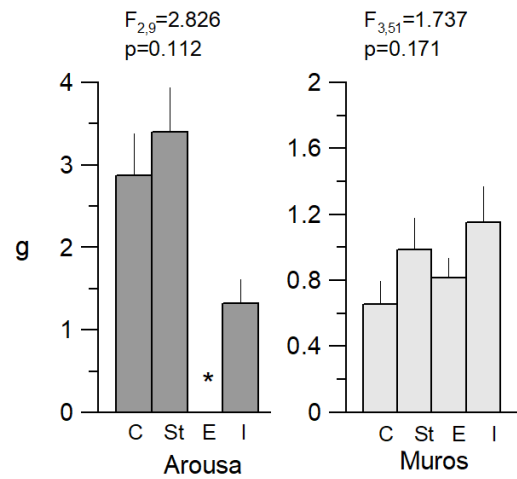
990

991 Figure 3. Number of germlings of *Fucus serratus* per disk at the end of the transplant experiment at the target
 992 locations (interior-I, origin-O and exterior-E) in the Rías de Arousa and Muros. In origin locations, stacked
 993 grey bars shown the germling counts after subtracting the new settlers recorded on control discs. Means \pm SE,
 994 n as indicated.

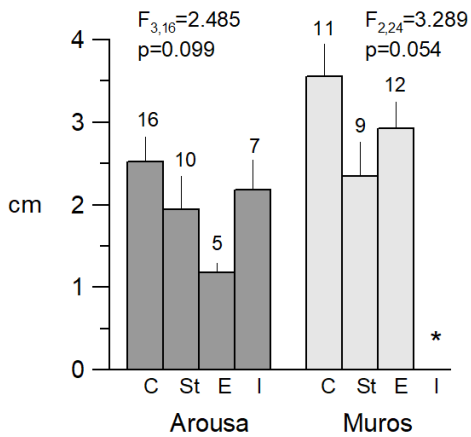
a) First Trial, Elongation



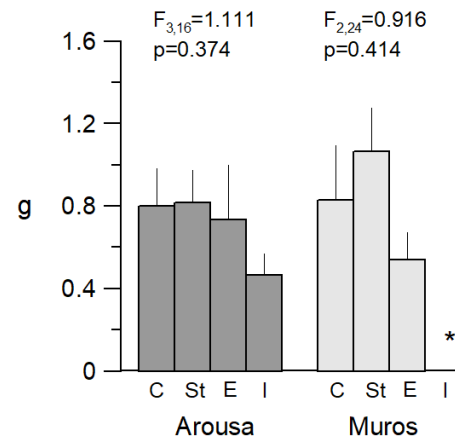
b) First Trial, Dry weight



c) Second Trial, Elongation



d) Second Trial, Dry weight

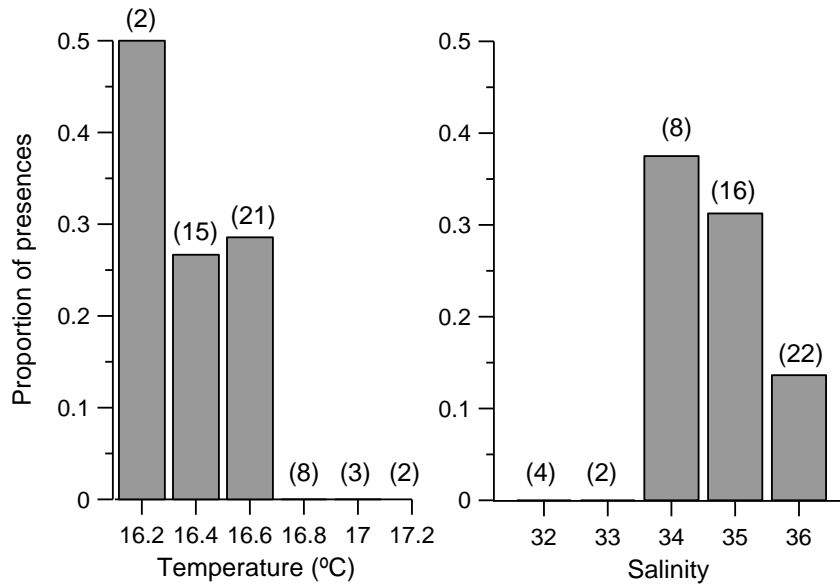


995

996 Figure 4. Elongation (cm) and final dry weights (g) in the transplant treatments with juveniles in Ría de
 997 Arousa and Ría de Muros in both trials. Treatment abbreviations: C = controls, St = self-transplants, E =
 998 exterior transplants, I = interior transplants. Asterisks indicate those treatments where all data are
 999 missing. Means \pm SE, n as indicated. The F tests and p-values of one-way ANOVAs are also shown. Data
 1000 within treatments were balanced for analyses (First Trial, Ría de Arousa n=4, Ría de Muros n=11; Second
 1001 Trial, Ría de Arousa n=5, Ría de Muros, n = 9).

1002

1003



1004

1005

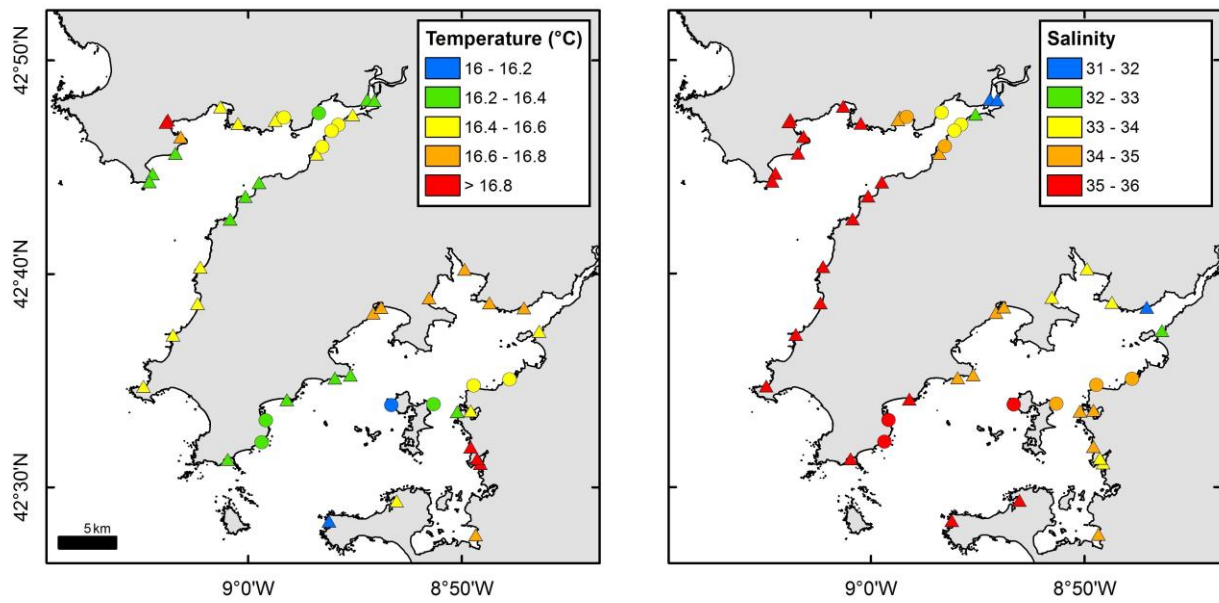
1006 Figure 5. Histograms showing the proportion of *F.serratus* presences for the environmental predictors

1007 included in the best species distribution model: maximum autumn seawater temperature and mean salinity in

1008 January-February. Number of records are shown.

1009

1010



1011

1012 Figure 6. Maps showing the values of the explanatory variables included in the best species distribution model
1013 (maximum sea temperature in autumn and mean salinity in January-February) at the studied locations.

1014 Circles/triangles indicate the sites with presence/absence of *F. serratus*.